

Quantitative dynamic-mode scanning force microscopy in liquid

B. W. Hoogenboom^{a)}

Institute of Physics, University of Basel, CH-4056 Basel, Switzerland and M. E. Müller Institute, Biozentrum, University of Basel, CH-4056 Basel, Switzerland

H. J. Hug

Institute of Physics, University of Basel, CH-4056 Basel, Switzerland and Swiss Federal Laboratories for Materials Testing and Research, EMPA, CH-8600 Dübendorf, Switzerland

Y. Pellmont and S. Martin

Institute of Physics, University of Basel, CH-4056 Basel, Switzerland

P. L. T. M. Frederix, D. Fotiadis, and A. Engel

M. E. Müller Institute, Biozentrum, University of Basel, CH-4056 Basel, Switzerland

(Received 10 January 2006; accepted 23 March 2006; published online 9 May 2006)

We describe a method to perform dynamic-mode scanning force microscopy in liquid with true atomic resolution. A frequency-modulation technique is used to maintain constant amplitude, phase, and frequency shift of the cantilever oscillation. As a consequence, the tip-sample interaction force is well defined and quantitative. The force sensitivity is demonstrated by imaging and deliberate bending of a peptide loop connecting transmembrane helices of the membrane protein bacteriorhodopsin. The experimental setup allows further enhancement of the force sensitivity by the use of small cantilevers. © 2006 American Institute of Physics. [DOI: 10.1063/1.2202638]

The scanning (or atomic) force microscope (SFM) is a versatile tool to image surfaces with up to atomic resolution in various environments. It allows the study of single biological molecules in their native (liquid) environment.¹ In such experiments, precise control of the tip-sample interaction force is a prerequisite to achieve sufficiently large signal-to-noise ratio without distortion of the sample. In addition, by a controlled variation of the interaction force, it is possible to distinguish flexible and stiff components of molecules.² To image and interpret these biologically relevant details, a quantitative control of the force is needed.

In liquid, the highest resolution—up to true atomic resolution³—has been obtained in constant-force mode. However, scanning a sample with a constant (vertical) force implies (lateral) friction forces which can damage delicate molecules, or detach them from the substrate. Furthermore, as a dc/low-frequency technique, constant-force mode is subject to drift, which makes precise control of the interaction force a difficult task. In dynamic mode, in contrast, lateral forces are minimized, and the (high-frequency) signal can easily be distinguished from (low-frequency) drift. A robust quantitative force control can be achieved using a frequency-modulation detection technique.⁴ Frequency-modulation scanning force microscopy (FM-SFM) has recently been shown to yield quantitative force measurements⁵ and images with true atomic resolution⁶ in liquid.

This letter describes how to perform high-resolution FM-SFM imaging in liquid with a well-defined, quantitative force. On mica, atomic-scale defects and a corrugation of 40 pm are clearly resolved. The precise control of the interaction forces is demonstrated by imaging a peptide loop between two transmembrane helices of bacteriorhodopsin, and by deliberately bending it.

When a cantilever oscillates in the vicinity of a sample surface, the gradient of the conservative tip-sample interac-

tion force leads to a shift Δf of the eigenfrequency f_0 of the cantilever. Dissipative forces damp the amplitude A of the oscillation, but do not change Δf . The conservative tip-sample interaction varies over the oscillation cycle of the cantilever. It can be quantitatively determined, provided that Δf is known as a function of the tip-sample distance and that A is kept constant by adjusting the driving force.^{7,8} In an FM-SFM experiment, Δf can be measured as the output of a phase-locked loop (PLL) that keeps the phase constant at $-\pi/2$ by adjusting the oscillation frequency.

Our SFM contains a Fabry-Perot interferometer with a 3 μm spot size and $<3 \text{ fm}/\sqrt{\text{Hz}}$ noise floor,⁹ and a rigid fluid cell with cantilever, both mounted in a home-built unit on top of a commercial microscope base (Veeco Multimode, with E scanner). The microscope is operated with a digital FM-SFM controller (SwissProbe).

The cantilever oscillation is driven by a piezoactuator on which the cantilever support chip is mounted. This way of driving the cantilever avoids adding complexity to the cantilever itself. However, due to the presence of mechanical resonances other than that of the cantilever, both the amplitude and the phase of the driven cantilever oscillation deviate from the harmonic-oscillator response (Fig. 1). This is a par-

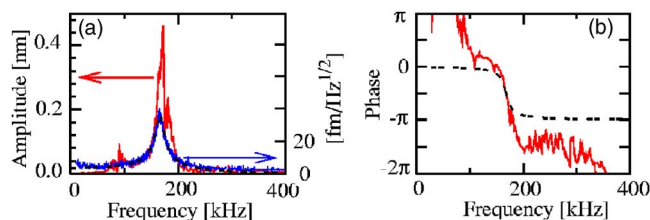


FIG. 1. (Color online) Red, solid curves (left axes): (a) amplitude and (b) phase of a cantilever in buffer solution, actuated by the piezostack on which the cantilever is mounted. Blue, solid curve [right axis in (a)]: thermal noise of the cantilever. The black, dashed curve overlaying the thermal noise in (a) is a harmonic-oscillator fit. The phase corresponding to this fit is depicted as a black, dashed curve in (b).

^{a)}Electronic mail: Bart.Hoogenboom@unibas.ch

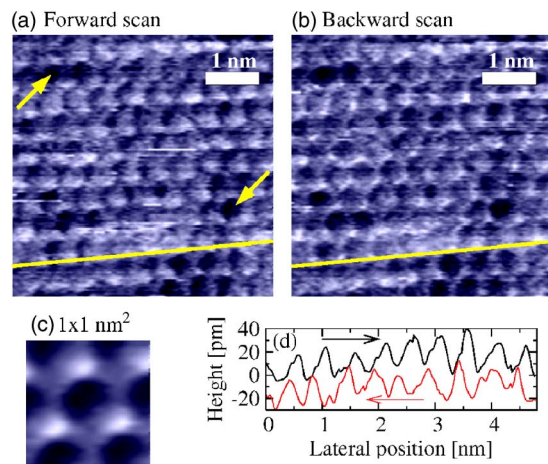


FIG. 2. (Color online) SFM imaging of the cleaved (001) surface of muscovite mica in buffer solution, with constant frequency shift $\Delta f = 110$ Hz and constant amplitude $A = 0.64$ nm. (a) Forward and (b) backward scan (fast scan axis: horizontal). The vertical scale (black to white) is 70 pm. A background plane has been subtracted from the data. The arrows point to two examples of atomic-scale defects, visible in both the forward and the backward scan. (c) Correlation-averaged image of the unit cell (vertical scale: 40 pm). (d) Line sections along the yellow lines in (a) and (b). The arrows indicate the fast scan direction (forward/backward) for both curves. The offset of the vertical scale is arbitrary.

ticular problem of dynamic-mode operation in liquid, where the quality factor of the cantilever $Q \leq 10$ (compared to $\geq 10^4$ in vacuum), i.e., comparable to or smaller than the quality factors of other mechanical resonances in the system.¹⁰

Since the measurement of Δf relies on the phase of the cantilever oscillation, it is important to verify that the measured phase near f_0 follows the harmonic-oscillator phase response over at least some kilohertz. To this end, the harmonic-oscillator amplitude response of the cantilever is determined by measuring the thermal noise of the cantilever, as is shown in Fig. 1(a). The noise floor of the measurement is sufficiently low to allow an accurate fit,⁴ here yielding $f_0 = 167$ kHz, $Q = 10$, and $k = 1.3 \times 10^2$ N/m (cantilever: Nanosensors NCH). From this fit, the expected phase response of the cantilever is derived [dashed line in Fig. 1(b)]. Near f_0 , it closely matches the measured phase of the piezo-driven cantilever (as has been verified for all cantilevers used here), justifying a quantitative interpretation of the measured Δf .

Another problem related to the small Q is the reduced force sensitivity: The thermal noise of the cantilever leads to a minimum detectable force gradient—averaged over the full oscillation—proportional to $1/\sqrt{Q}$.⁴ The sensitivity for short-range forces, however, can be maximized by working at small (≤ 1 nm) amplitudes.⁶ Our Fabry-Perot interferometer, with a noise floor of < 3 fm/ $\sqrt{\text{Hz}}$ [see Fig. 1(a)], is particularly suited for this.

Figure 2 shows constant- Δf images of mica obtained with the cantilever characterized in Fig. 1, recorded in a buffer solution (150 mM KCl, 20 mM Tris-HCl, pH=7.8) that is common for imaging biological samples in constant-force mode.² The scan speed is low (here 5.8 nm/s), to make sure that the sample corrugation (periodicity 0.5 nm) appears well within the bandwidth of the feedback loops (typically between 100 and 1000 Hz). Thus (i) the feedback of the PLL can keep the phase constant, such that the Δf output of the

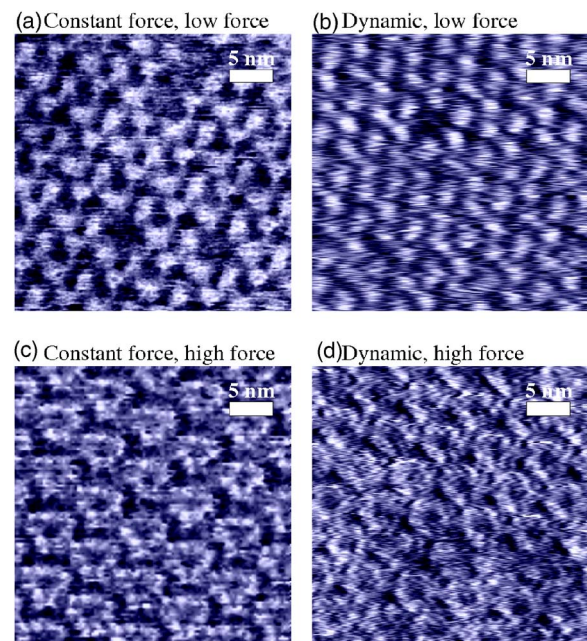


FIG. 3. (Color online) Constant-force mode and dynamic mode (with constant frequency shift and amplitude) images of the cytoplasmic surface of purple membrane in aqueous solution. The data have been flattened. (a) Force ≤ 0.1 nN, and vertical scale (black to white) 0.67 nm. (b) $\Delta f = 400$ Hz, $A = 0.64$ nm, $\langle F \rangle = 0.3$ nN, and vertical scale 0.50 nm. (c) Force ≈ 0.3 nN, and vertical scale 0.43 nm. (d) $\Delta f = 800$ Hz, $A = 1.0$ nm, $\langle F \rangle = 0.8$ nN, and vertical scale 0.31 nm.

PLL reflects the true Δf ; (ii) the amplitude feedback can keep the amplitude A constant; and (iii) the feedback controlling the vertical sample position can keep Δf constant. With respect to these points, our images differ from the atomic-resolution images of Ref. 6. For all measurements, Δf and A can be found in the figure captions.

On mica, we then observe a corrugation of 40 pm and atomic-scale defects (Fig. 2). The measured corrugation of 40 pm represents an equi- Δf surface, and the positive Δf is due to a (small) repulsive tip-sample interaction force. This force can be quantified, here $F_{\text{max}} = 0.5$ nN, following the procedure described below for experiments on bacteriorhodopsin.

The same experimental setup can also be used to image biological samples applying well-defined, quantitative forces. As a test sample, the cytoplasmic side of purple membrane has been imaged in aqueous solution. Purple membrane contains bacteriorhodopsin (BR) trimers, packed into a trigonal two-dimensional (2D) lattice.

Constant-force SFM topographs of purple membrane have shown that the surface structure of BR strongly depends on the interaction force.² When imaged at minimum force, i.e., ≤ 0.1 nN, the most prominent feature of BR is the bulky peptide loop connecting the transmembrane helices E and F . At higher forces, this loop bends, and otherwise hidden shorter loops become visible, giving BR trimers a flat and donutlike appearance. For comparison with the dynamic-mode images discussed below, Figs. 3(a) and 3(c) show constant-force images at ≤ 0.1 nN and at about 0.3 nN, respectively. The cantilever spring constant is about 0.1 N/m; the scan speed is 600 nm/s. The imaging conditions are similar to Ref. 2.

In our FM-SFM setup, BR has been imaged in buffer solution (25 mM MgCl_2 , 150 mM KCl, 20 mM Tris-HCl,

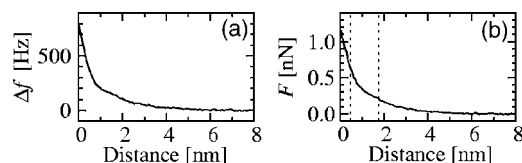


FIG. 4. (a) Frequency shift Δf and (b) corresponding interaction force F as a function of distance from a purple membrane sample. Zero distance corresponds to the closest approach of the cantilever to the sample during an oscillation with $\Delta f=800$ Hz. Further conditions correspond to Fig. 3(b). The dashed, vertical lines in (b) indicate the shortest and longest distance between the tip and the sample for $\Delta f=400$ Hz.

pH=7.8), using cantilevers with spring constants ranging from 10 to over 100 N/m. For the dynamic-mode (FM-SFM) data in Figs. 3(b) and 3(d), the cantilever characteristics are $f_0=107$ kHz, $Q=6.2$, and $k=46$ N/m (cantilever: Nanosensors NCH). The scan speed is 250 nm/s. The imaging conditions are stable, i.e., no adjustment of parameters is required while recording an image. This is a clear improvement with respect to constant-force mode, where the operator continuously adjusts the deflection setpoint to compensate for drift.

To compare the images taken in FM-SFM to data acquired in constant-force mode, the dependence of Δf on the tip-sample distance has been measured [Fig. 4(a)]. Using a procedure described in Ref. 8, the interaction force can be derived from this Δf -distance curve. Note that the horizontal scale of the force-distance curve in Fig. 4(b) corresponds to the tip-sample distance at the lower turning point of the oscillating cantilever. Hence, for a constant Δf , the force varies between a maximum value at the lower, and a minimum value at the upper turning point. Both on mica and on BR, the measured Δf -distance curves do not show any significant dependence on the lateral position within the displayed images. This implies that F_{\max} , F_{\min} , and $\langle F \rangle$ are well defined within the scanned sample area. In Fig. 3(b), the forces are $F_{\max}=0.6$ nN, $F_{\min}=0.2$ nN, and $\langle F \rangle=0.3$ nN; and in Fig. 3(d), $F_{\max}=1.5$ nN, $F_{\min}=0.3$ nN, and $\langle F \rangle=0.8$ nN.

FM-SFM thus leads to similar images as constant-force mode, even at higher vertical forces. This strongly suggests that the fast vertical oscillation of the cantilever reduces the lateral friction force on the molecules. The reduction of lateral forces, the small sensitivity to drift, and the ability to precisely measure and adjust the tip-sample interaction, make FM-SFM highly suited to study single biological molecules, also when they are not arranged in 2D crystalline structures.

Further optimization of dynamic-mode imaging can be achieved by the use of small cantilevers.^{11,12} The setup described in this letter uses a highly sensitive small-spot deflection detector⁹ and relies on piezoactuation of the cantilever, not requiring any added complexity and mass to the cantilever itself. It is therefore well adapted to optimally benefit from the high eigenfrequencies (for relatively low spring constants) of small cantilevers, thus further reducing noise or enhancing the measurement speed.

This work has been supported by the Swiss Top Nano 21 program and by the NCCR Nanoscale Science.

¹A. Engel and D. J. Müller, *Nat. Struct. Biol.* **7**, 715 (2000).

²D. J. Müller, G. Büldt, and A. Engel, *J. Mol. Biol.* **249**, 239 (1995).

³F. Ohnesorge and G. Binnig, *Science* **260**, 1451 (1993).

⁴T. R. Albrecht, P. Grütter, D. Horne, and D. Rugar, *J. Appl. Phys.* **69**, 668 (1991).

⁵T. Uchihashi, M. J. Higgins, S. Yasuda, S. P. Jarvis, S. Akita, Y. Nakayama, and J. E. Sader, *Appl. Phys. Lett.* **85**, 3575 (2004).

⁶T. Fukuma, K. Kobayashi, K. Matsushige, and H. Yamada, *Appl. Phys. Lett.* **87**, 034101 (2005).

⁷F. J. Giessibl, *Phys. Rev. B* **56**, 16010 (1997).

⁸J. E. Sader and S. P. Jarvis, *Appl. Phys. Lett.* **84**, 1801 (2004).

⁹B. W. Hoogenboom, P. L. T. M. Frederix, J. L. Yang, S. Martin, Y. Pellmont, M. Steinacher, S. Zäch, E. Langenbach, H.-J. Heimbeck, A. Engel, and H. J. Hug, *Appl. Phys. Lett.* **86**, 074101 (2005).

¹⁰T. E. Schäffer, J. P. Cleveland, F. Ohnesorge, D. A. Walters, and P. K. Hansma, *J. Appl. Phys.* **80**, 3622 (1996).

¹¹M. B. Viani, T. E. Schäffer, A. Chand, M. Rief, H. E. Gaub, and P. K. Hansma, *J. Appl. Phys.* **86**, 2258 (1999).

¹²J. L. Yang, M. Despont, U. Drechsler, B. W. Hoogenboom, P. L. T. M. Frederix, S. Martin, A. Engel, P. Vettiger, and H. J. Hug, *Appl. Phys. Lett.* **86**, 134101 (2005).